Biomedical Optics EXPRESS

Measurements of multiphoton action cross sections for multiphoton microscopy

Li-Chung Cheng,[1,2] Nicholas G. Horton,[2] Ke Wang,[3] Shean-Jen Chen,[4,5] and Chris Xu[2,*]

[1]*Department of Photonics, National Cheng Kung University, Tainan 701, Taiwan*
[2]*School of Applied and Engineering Physics, Cornell University, Ithaca, New York 14853, USA*
[3]*Key Laboratory of Optoelectronic Devices and Systems of Ministry of Education and Guangdong Province, College of Optoelectronic Engineering, Shenzhen University, Shenzhen 518060 China*
[4]*Department of Engineering Science, National Cheng Kung University, Tainan 701, Taiwan*
[5]*Advanced Optoelectronic Technology Center, National Cheng Kung University, Tainan 701, Taiwan*
[*]*chris.xu@cornell.edu*

Abstract: We report quantitative measurements of two-, three-, and four-photon excitation action cross sections of several commonly used fluorophores and fluorescent proteins at three different excitation wavelengths of 800 nm, 1300 nm, and 1680 nm. The measured cross section values are consistent with simple quantum mechanic estimations. These values indicate that the optimum repetition rate for deep tissue 3-photon microscopy is approximately 1 to 2 MHz. We further demonstrate that it is feasible to perform 4-photon fluorescence microscopy of GFP labeled microglia in mouse brain in vivo at 1700 nm. 4-photon excitation increases the accessibility of fluorophores at the long wavelength spectral window of 1700 nm.

OCIS codes: (190.0190) Nonlinear optics; (190.4180) Multiphoton processes.

References and links

1. D. Kobat, M. E. Durst, N. Nishimura, A. W. Wong, C. B. Schaffer, and C. Xu, "Deep tissue multiphoton microscopy using longer wavelength excitation," Opt. Express **17**(16), 13354–13364 (2009).
2. D. Kobat, N.G. Horton, and C. Xu, "In vivo two-photon imaging of cortical vasculature in mice to 1.5-mm depth with 1280-nm excitation," CLEO, postdeadline paper, PDPB3(2011).
3. M. Balu, T. Baldacchini, J. Carter, T. B. Krasieva, R. Zadoyan, and B. J. Tromberg, "Effect of excitation wavelength on penetration depth in nonlinear optical microscopy of turbid media," J. Biomed. Opt. **14**(1), 010508 (2009).
4. V. Andresen, S. Alexander, W. M. Heupel, M. Hirschberg, R. M. Hoffman, and P. Friedl, "Infrared multiphoton microscopy: subcellular-resolved deep tissue imaging," Curr. Opin. Biotechnol. **20**(1), 54–62 (2009).
5. D. Kobat, N. G. Horton, and C. Xu, "In vivo two-photon microscopy to 1.6-mm depth in mouse cortex," J. Biomed. Opt. **16**(10), 106014 (2011).
6. P. Theer and W. Denk, "On the fundamental imaging-depth limit in two-photon microscopy," J. Opt. Soc. Am. A **23**(12), 3139–3149 (2006).
7. N. G. Horton, K. Wang, D. Kobat, C. G. Clark, F. W. Wise, C. B. Schaffer, and C. Xu, "In vivo three-photon microscopy of subcortical structures within an intact mouse brain," Nat. Photonics **7**(3), 205–209 (2013).
8. C. Xu and W. W. Webb, "Measurement of two-photon excitation cross sections of molecular fluorophores with data from 690 to 1050 nm," J. Opt. Soc. Am. B **13**(3), 481–491 (1996).
9. C. Xu, W. Zipfel, J. B. Shear, R. M. Williams, and W. W. Webb, "Multiphoton fluorescence excitation: New spectral windows for biological nonlinear microscopy," Proc. Natl. Acad. Sci. U.S.A. **93**(20), 10763–10768 (1996).
10. M. A. Albota, C. Xu, and W. W. Webb, "Two-photon fluorescence excitation cross sections of biomolecular probes from 690 to 960 nm," Appl. Opt. **37**(31), 7352–7356 (1998).
11. N. S. Makarov, M. Drobizhev, and A. Rebane, "Two-photon absorption standards in the 550-1600 nm excitation wavelength range," Opt. Express **16**(6), 4029–4047 (2008).
12. J. Mütze, V. Iyer, J. J. Macklin, J. Colonell, B. Karsh, Z. Petrášek, P. Schwille, L. L. Looger, L. D. Lavis, and T. D. Harris, "Excitation spectra and brightness optimization of two-photon excited probes," Biophys. J. **102**(4), 934–944 (2012).
13. G. A. Blab, P. H. M. Lommerse, L. Cognet, G. S. Harms, and T. Schmidt, "Two-photon excitation action cross-sections of the autofluorescent proteins," Chem. Phys. Lett. **350**(1-2), 71–77 (2001).
14. M. Drobizhev, S. Tillo, N. S. Makarov, T. E. Hughes, and A. Rebane, "Absolute Two-Photon Absorption Spectra and Two-Photon Brightness of Orange and Red Fluorescent Proteins," J. Phys. Chem. B **113**(4), 855–859 (2009).

#216528 - $15.00 USD Received 7 Jul 2014; revised 26 Aug 2014; accepted 26 Aug 2014; published 4 Sep 2014

15. M. Drobizhev, N. S. Makarov, S. E. Tillo, T. E. Hughes, and A. Rebane, "Two-photon absorption properties of fluorescent proteins," Nat. Methods **8**(5), 393–399 (2011).
16. B. Zysset, P. Beaud, and W. Hodel, "Generation of optical solitons in the wavelength region 1.37–1.49 mm," Appl. Phys. Lett. **50**(16), 1027–1029 (1987).
17. K. Wang and C. Xu, "Tunable high-energy soliton pulse generation from a large mode- area fiber and its application to third harmonic generation microscopy," Appl. Phys. Lett. **99**(7), 071112 (2011).
18. C. Xu and W. W. Webb, *Topics in Fluorescence Spectroscopy*, Vol. 5 (Springer, 1997), Chap. 11.
19. T. Bolmont, F. Haiss, D. Eicke, R. Radde, C. A. Mathis, W. E. Klunk, S. Kohsaka, M. Jucker, and M. E. Calhoun, "Dynamics of the microglial/amyloid interaction indicate a role in plaque maintenance," J. Neurosci. **28**(16), 4283–4292 (2008).
20. G. Olivié, D. Giguère, F. Vidal, T. Ozaki, J.-C. Kieffer, O. Nada, and I. Brunette, "Wavelength dependence of femtosecond laser ablation threshold of corneal stroma," Opt. Express **16**(6), 4121–4129 (2008).
21. I.-H. Chen, S.-W. Chu, C.-K. Sun, P.-C. Cheng, and B.-L. Lin, "Wavelength dependent damage in biological multi-photon confocal microscopy: a micro-spectroscopic comparison between femtosecond Ti:sapphire and Cr:forsterite laser sources," Opt. Quantum Electron. **34**(12), 1251–1266 (2002).
22. Y. Fu, H. Wang, R. Shi, and J.-X. Cheng, "Characterization of photodamage in coherent anti-Stokes Raman scattering microscopy," Opt. Express **14**(9), 3942–3951 (2006).
23. W. Mittmann, D. J. Wallace, U. Czubayko, J. T. Herb, A. T. Schaefer, L. L. Looger, W. Denk, and J. N. D. Kerr, "Two-photon calcium imaging of evoked activity from L5 somatosensory neurons in vivo," Nat. Neurosci. **14**(8), 1089–1093 (2011).
24. D. Ouzounov, N. Horton, T. Wang, D. Feng, N. Nishimura, C. Xu, "In Vivo Three-photon Calcium Imaging of Brain Activity from Layer 6 Neurons in Mouse Brain," CLEO, postdeadline paper, STh4C.2 (2014).

1. Introduction

Multiphoton microscopy (MPM) has several advantages in *in vivo* imaging of biological tissues. Because two- or three-photon excited fluorescence increases quadratically or cubically with the excitation intensity, the fluorescence, and the potential photobleaching and photodamage related to nonlinear fluorescence excitation, are all confined to the vicinity of the focus. This spatial localization not only provides intrinsic three-dimensional resolution in fluorescence microscopy but also allows large area detectors to capture the signal. Even multiply scattered fluorescence photons contribute equally to the image formation, in contrast with confocal microscopy where the unscattered photons form the confocal image. This efficient detection of fluorescence photons, combined with the relatively deep penetration of IR excitation light in most biological preparations, enables MPM to image deep into turbid biological specimens. Research on longer wavelength MPM (mostly at ~1300 nm) for deep tissue imaging opened a new direction [1–5]. A record 1.6-mm penetration depth was achieved in mouse cortex *in vivo* [5], nearly double the previous depth limit. Nonetheless, the fundamental depth limit for high-resolution two-photon microscopy (2PM) is the signal-to-background ratio (SBR) of the excitation in scattering biological tissue [5,6]. As the penetration depth increases, the background, which is defined as the fluorescence excitation outside the focal volume, increases exponentially and eventually overwhelms the signal from the focus. Recently, Horton et al. demonstrated deep tissue three-photon fluorescence microscopy (3PM) of mouse brain *in vivo* at the 1700 nm spectral window [7]. 3PM not only improves the SBR by several orders of magnitude but also enables the excitation of conventional fluorophores and fluorescent proteins using the longer excitation wavelength. The combination of 3-photon excitation (3PE) and the longer excitation spectral windows (i.e., 1300 nm and 1700 nm) is promising for *in vivo* deep tissue microscopy.

Multiphoton excitation cross-sections are essential parameters for MPM. In the past two decades, the two-photon excitation (2PE) cross sections of many common fluorophores [8–12] and fluorescent proteins [13–15] were measured. These data provide a reliable database for two-photon fluorescence microscopy. However, 3PE cross sections are known for only a handful of fluorophores, and there is hardly any quantitative measurement of three- or four-photon excitation (4PE) cross section of fluorophores in the long wavelength excitation windows of 1300 nm and 1700 nm that are perhaps most suited for deep tissue penetration. In this paper, we report measurements of two-, three-, and four-photon excitation action cross sections of common fluorophores (fluorescein and Sulforhodamine-101) and wild-type green fluorescent protein (wtGFP) by using three different excitation wavelengths, 800 nm, 1300 nm, and 1700 nm. We demonstrate 4-photon fluorescence microscopy of GFP labeled brain

#216528 - $15.00 USD Received 7 Jul 2014; revised 26 Aug 2014; accepted 26 Aug 2014; published 4 Sep 2014

tissue *in vivo* using 1700 nm excitation. We further discuss the implications of the measured cross section values on MPM, particularly in the context of deep tissue microscopy.

2. Multi-photon excitation theory

We determined the action cross section of two-, three-, and four-photon excitation by measuring the fluorescence signal. We expanded the laser beams to overfill the back aperture of the objective lens (*NA* = 0.3). As a result, we achieved approximately diffraction-limited illumination of the sample. Following the multiphoton excitation analysis of Xu et al. [9], we can obtain the relation between time-averaged fluorescence photon flux $\left\langle F^{(n)}(t)\right\rangle$ and incident power $P(t)$ under two-, three-, and four-photon excitation, in the thick sample limit:

$$\left\langle F^{(n)}(t)\right\rangle = \frac{1}{n}\frac{g_p^{(n)}}{(f\tau)^{n-1}}\phi\eta\sigma_n C n_0 \frac{a_n (NA)^{2n-4}\left\langle P(t)\right\rangle^n}{8\pi^{3-n}\lambda^{2n-3}}, \tag{1}$$

where n is the number of photons absorbed, f is the laser repetition rate, τ is the laser pulse width, ϕ is the system collection efficiency, η is the fluorescence quantum efficiency, C is the concentration of the fluorophore, and σ_n is the n-photon absorption cross section, λ is the excitation wavelength in vacuum, and $a_2 = 64$, $a_3 = 28.1$, $a_4 = 18.3$. $g_p^{(n)}$ is the n^{th}-order temporal coherence of the excitation source:

$$g_p^{(n)} = \tau^{n-1}\frac{\int_{-T/2}^{T/2} I_0^n(t)dt}{\left[\int_{-T/2}^{T/2} I_0(t)dt\right]^n}, \tag{2}$$

which is a dimensionless quantity. $T = 1/f$ is the period of the laser pulse. $I_0(t)$ is the time-dependent intensity at the focus. For Gaussian temporal profile pulse $g_p^{(2)} = 0.664$, $g_p^{(3)} = 0.51$, and $g_p^{(4)} = 0.415$, and for hyperbolic-secant-squared pulse $g_p^{(2)} = 0.587$, $g_p^{(3)} = 0.413$, and $g_p^{(4)} = 0.312$. We note that, in the thick sample limit, the generated fluorescence depends on the *NA* in both three- and four-photon excitation. By assuming a certain pulse shape, we can measure the pulse width and $g_p^{(n)}$. All other quantities excluding (σ) in the above equations can also be quantitatively measured, from which we can get the action cross section ($\eta\sigma$).

3. Experimental setup for measuring the multiphoton cross sections

In this measurement, we used three different light sources for two-, three-, and four-photon excitation. A Ti:sapphire oscillator at 800 nm was used for measuring two-photon action cross sections of fluorescein, sulforhodamine-101 (SR101), and wtGFP. An optical parametric amplifier (OPA, OPA9850, Coherent, pumped by a chirped pulse amplification system, RegA9050, Coherent) at 1300 nm was used for measuring the three-photon action cross sections of fluorescein and wtGFP. A femtosecond pulsed source at 1680 nm based on soliton self-frequency shift (SSFS) in a photonic crystal (PC) rod [16,17] was used for measuring three-photon action cross section of SR101 and four-photon action cross sections of fluorescein and wtGFP. The experiment setup is shown in Fig. 1. The excitation power at the sample was adjusted by a half-wave plate and a polarization beam splitter. The excitation beams were expanded to completely overfill the back aperture of the objective lens (UPLFLN 0.3 NA/10X, Olympus) so that a diffraction-limited focus at the sample is achieved. The emitted fluorescence photons were collected in the epi-direction by the same objective lens. Different dichroic mirrors were used to separate the fluorescence from the excitation beams.

#216528 - $15.00 USD Received 7 Jul 2014; revised 26 Aug 2014; accepted 26 Aug 2014; published 4 Sep 2014

After a set of proper emission filters, the generated fluorescence was detected by a photomultiplier tube (PMT, HC125-2, HAMAMATSU), and recorded by a photon counter (SR400, Stanford Research Systems).

Equation (1) shows that three- and four-photon excitation cross sections depend on the second and fourth power of *NA*, respectively. It is important to determine the excitation *NA* of the objective lens experimentally. Here we used two methods to experimentally determine the *NA* of the objective lens. In the first approach, we measured the beam spot size using the knife-edge method at several axial positions to determine the divergence (or convergence) angle of the excitation beam after the objective lens. The *NA*s measured by the knife-edge method are 0.261, 0.262 and 0.258 at 800 nm, 1300 nm and 1680 nm, respectively. In the second approach, we measured the two-photon axial response of the objective lens at 800 nm by axially scanning a rhodamine B thin film (thickness ~0.5 μm). By fitting the axial response curve, we found the *NA* is 0.257 at 800 nm, which is in good agreement with the *NA* obtained by the knife-edge method. We used the *NA* of 0.26 in our cross section measurement. The discrepancy between the measured and the specified *NA*s may be due to the fact that the objective lens is designed for UV and visible wavelength.

For sample preparations, we dissolved fluorescein (Acros Organics) in H_2O and NaOH. The solution has a pH value of 13 and a concentration of 10.9 μM, and was used as our standard calibration sample. SR101 (Santa Cruz Biotechnology) was dissolved in phosphate buffered saline (PBS) to 7.6 μM. A stock solution of 37.3 μM wtGFP was directly obtained from Abcam. The concentrations of fluorescein and SR101 were confirmed by measuring the absorption in a spectrophotometer (Cary 50 UV-VIS, Varian) using the known one-photon extinction coefficient.

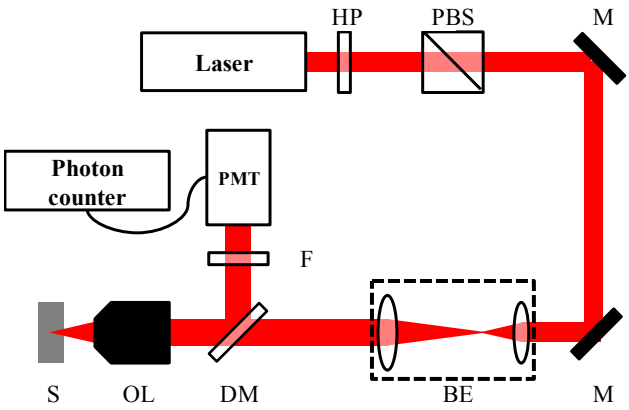

Fig. 1. Experiment setup for measuring two-, three-, and four-photon excitation cross section. HP: half-wave plate. PBS: polarization beam splitter. M: mirror. BE: beam expander. DM: dichroic mirror. OL: objective lens. S: sample. F: emission filter. PMT: photomultiplier tube.

4. Cross section measurement results

Before measuring the action cross sections, we first used the known two-photon cross section of fluorescein as a standard to calibrate the fluorescence collection efficiency of the system. Such a calibration also works well for wtGFP since the fluorescence emission wavelength of GFP is similar to that of fluorescein. For SR101, we combined this calibration with our measurements of the optical components (e.g., filters, dichroic mirror, PMT response) to obtain the collection efficiency of the system. Figure 2 shows the dependence of fluorescence intensities on the excitation photon flux density (plotted on logarithmic scales). Red, blue, and black squares represent, respectively, the fluorescence of 10.9 μM solution of fluorescein, 37.3 μM solution of wtGFP, and 7.6 μM solution of SR101. The solid lines are linear fits to the experimental results. The slopes of the lines are indicated in each figure, which confirm

#216528 - $15.00 USD Received 7 Jul 2014; revised 26 Aug 2014; accepted 26 Aug 2014; published 4 Sep 2014

that the generated fluorescence is due to two- [Fig. 2(a)], three- [Fig. 2(b)] and four-photon [Fig. 2(c)] excitation. Based on Eq. (1), we can obtain two-, three-, and four-photon action cross sections of fluorescein, wtGFP, and SR101. The results are summarized in Table 1. The measured two-photon action cross section of SR101 is in good agreement with the value reported previously [12]. The measured two-photon action cross section of wtGFP (21.6 GM at 800 nm, 1 GM = 10^{-50} cm^4s/photon) appears to be larger than that reported previously, which has a value of 12 GM at 810 nm [15]. The estimated measurement uncertainty (~30%), which is mainly due to the uncertainty in the determination of the collection efficiency of the system, is similar to previously published cross section works [8, 9] since similar methods are used in this experiment. These data will serve as a useful guide for multiphoton imaging.

Multiphoton excitation processes require two or more photons to interact simultaneously with the molecule. Although the multiphoton transition strength consists of contributions from all available quantum states as possible intermediate states, the single intermediate state (SIS) approximation can be used to give an order-of-magnitude estimation. As shown by Xu et al [18], the SIS approximation predicts that the two-, three-, and four-photon excitation cross sections are on the order of 10^{-49} cm^4s/photon, 10^{-82} cm^6(s/photon)^2, and 10^{-115} cm^8(s/photon)^3, respectively. Although we did not measure the spectral variation of the excitation cross section (i.e., the excitation spectra), our measurement results nonetheless fall within one order of magnitude of these simple estimates. Due to the limited spectral bandwidth of the long wavelength windows (~150 nm at 1300 nm and 1700 nm), however, we do not expect the 3- and 4-photon cross section values to vary dramatically, particularly given the large spectral bandwidth (~40 nm) of the excitation pulse.

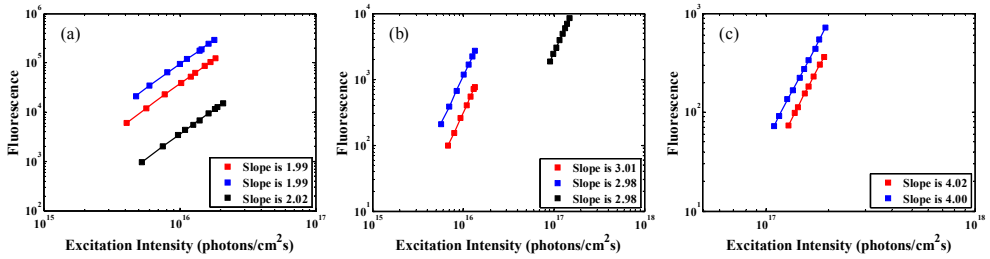

Fig. 2. Logarithmic plots of the dependence of (a) two-, (b) three-, and (c) four-photon-excited fluorescence on excitation intensity for fluorescein (red square), wtGFP (blue square), and SR101 (black square). The slopes are indicated in the lower-right corner of each figure.

Table 1. Two-, three-, and four-photon action cross sections of fluorescein, wtGFP and SR101

	$\eta\sigma_2$ 10^{-50} cm^4s/photon	$\eta\sigma_3$ 10^{-84} cm^6(s/photon)^2	$\eta\sigma_4$ 10^{-116} cm^8(s/photon)^3
Fluorescein	32.8 at 800 nm [10]	16.3 at 1300 nm	10.5 at 1680 nm
wtGFP	21.6 at 800 nm	15.9 at 1300 nm	4.9 at 1680 nm
SR101	20.6 at 800 nm	65.5 at 1680 nm	

5. 4PM of GFP labeled microglia *in vivo*

To demonstrate the feasibility of 4-photon fluorescence microscopy (4PM), the 1700 nm source was coupled to a multiphoton microscope. The microscope setup was similar to that described by Horton [7]. We imaged the brain of a male B6.129P-Cx3cr1 mouse (8 months old, The Jackson Laboratory) *in vivo* (Fig. 3). This mouse expresses EGFP within microglia. Figure 3(d) shows the characteristic features of microglia [19], and Fig. 3(f) shows that there is a clear separation between 4PM and the THG signal. Animal procedures were reviewed and approved by the Cornell Institutional Animal Care and Use Committee. Animals were prepared using the methods described by [5].

#216528 - $15.00 USD Received 7 Jul 2014; revised 26 Aug 2014; accepted 26 Aug 2014; published 4 Sep 2014

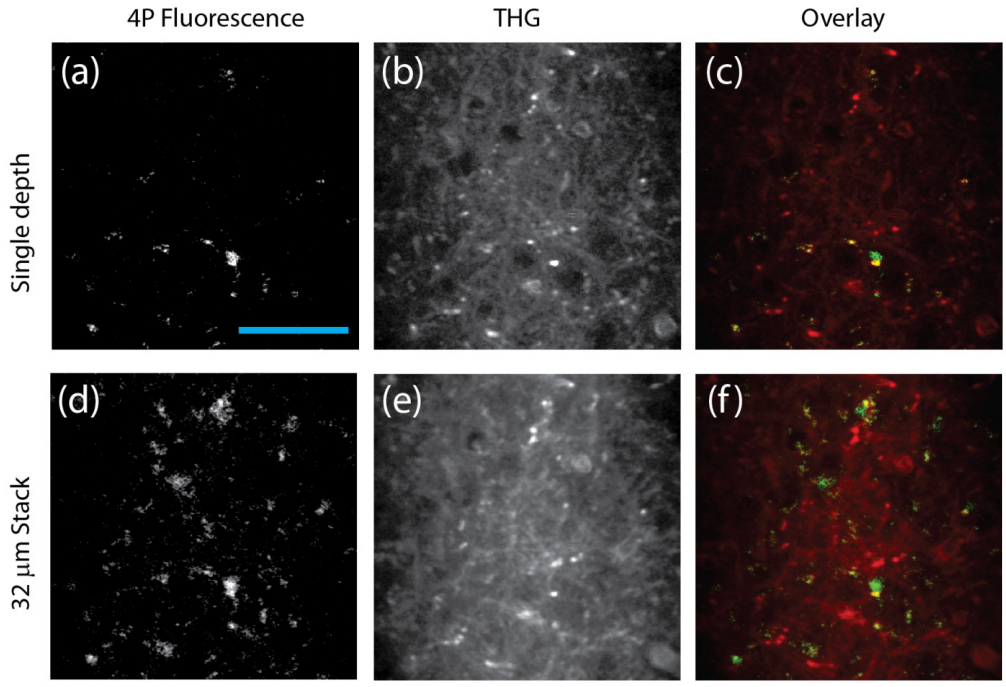

Fig. 3. 4PM and THG images of a mouse brain in vivo. (a-c): 2-frame averaging at a depth of 472 µm below the surface of the brain. (d-f): Average intensity of a 32 µm stack (2 frames per depth, 4 µm step size) ranging from 456 to 484 µm below the surface of the brain. The acquisition time was 4 seconds per frame, and the average power was 23 mW (repetition rate 1.3 MHz) on the brain surface. The scale bar is 50 µm.

6. Discussion

The measured multiphoton cross sections provide useful guidelines for MPM, particularly for the development of excitation sources for deep tissue imaging. For a given pulse width (typically ~100 fs for MPM), the pulse energy and repetition rate of the excitation source are constrained by the fluorophore cross section, which sets the maximum pulse energy at the focus, and tissue photodamage, that limits both the average power at the sample surface and the maximum pulse energy at the focus. Under short-pulse excitation, fluorescence saturates at the limit of one transition per pulse per fluorophore. Following [8] the saturation excitation power can be found by using $g_p^{(n)}\sigma_n\pi^n\tau\left\langle P(t)\right\rangle^n (NA)^{2n}\Big/\left[\lambda^{2n}(f\tau)^n\right]=1$. Given the estimated cross sections using the SIS approximation, the pulse energies for saturation of fluorescence excitation for two-, three-, and four-photon excitation are then approximately 1.1 nJ, 4.9 nJ, and 10.3 nJ, respectively, assuming 1700 nm excitation with 70 fs pulses and an excitation NA = 1.0. These pulse energies are below the ablative damage threshold for biological tissues [20] for wavelengths longer than 1000 nm, particularly for 2PE and 3PE. In addition, previous experiments demonstrated that longer excitation wavelengths reduce nonlinear tissue damage [21, 22]. Thus, linear absorption (i.e., the average power) is likely the main limitation when imaging deep into tissue using 1300 nm or 1700 nm excitation. Empirically, we found that there was no apparent photodamage when imaging the brain mouse *in vivo* at average powers approximately 140 mW and 40 mW, for 1300 nm and 1700 nm excitation, respectively. For maximum imaging depth, the excitation source should provide pulses with approximately the saturation pulse energy at the focus at various depths in the tissue, and at repetition rates that avoid sample heating. This argument shows that the optimum repetition rate for 3PM will be approximately 1 to 2 MHz when imaging deep into scattering tissue (e.g., for depth greater than three attenuation lengths). While such a repetition rate is

#216528 - $15.00 USD Received 7 Jul 2014; revised 26 Aug 2014; accepted 26 Aug 2014; published 4 Sep 2014

approximately a factor of 5 lower than the optimum source for 2PM, it is sufficient for imaging many dynamic biological events such as neuronal activity [23, 24]. Photobleaching is another potential concern, which may be highly dependent on the specific fluorescence probe. We have not observed adverse photobleaching effect when performing 3PM of GFP- and GCaMP6-labeled neurons in vivo using a laser source at the low repetition rate [24].

Ultrashort femtosecond pulses are essential for 3PM and 4PM due to the higher order nonlinear response (See Eq. (1). Pulse width less than 70 fs were used in previous deep tissue 3PM [7, 24]. While even shorter pulses will increase the excitation efficiency of 3PM, the dispersion of the optical elements must be carefully compensated for pulses significantly shorter than 50 fs.

Our results showed that it is feasible to perform 4PM at 1700 nm using an energetic femtosecond source at lower repetition rate. An obvious advantage of 4PM is to increase the spectral coverage of the excitation source, e.g., allowing the excitation of GFP at the 1700 nm spectral window. While 4PM will have even higher SBR when compared to 3PM, such an improvement is not practically meaningful currently since 3PM is no longer limited by the SBR at the imaging depth of 1 to 2 mm in the mouse brain [7]. Within this depth range, it is the signal-to-noise ratio, which is determined by the number of signal photons per pixel, limits the imaging speed and depth in 3PM and 4PM. Since higher pulse energy is required for efficient 4PE, the pulse repetition rate must be reduced to avoid sample heating, which further limits the imaging speed of 4PM when compared to 3PM.

7. Conclusion

We have quantitatively measured the 3PE and 4PE cross sections of several commonly used fluorophores in the long wavelength spectral windows of 1300 nm and 1700 nm. Our results showed that the 3PE and 4PE cross sections of these fluorophores are within an order of magnitude of previous estimations based on quantum mechanical perturbation theory. The measured cross section values indicate that the optimum repetition rate for deep tissue 3PM is approximately 1 to 2 MHz. We further demonstrated that it is feasible to perform 4PM of GFP labeled microglia *in vivo* at 1700 nm. 4PE increases the accessibility of fluorophores at the long wavelength spectral windows.

Acknowledgments

This work is partially funded by grant from the National Institutes of Health (NIH R01EB014873 to Chris Xu), and the National Science Foundation of China (No. 61475103), the Key Laboratory of Optoelectronic Devices and Systems of Ministry of Education and Guangdong Province, College of Optoelectronic Engineering, Shenzhen University (SZU, No. GD201401), and the Natural Science Foundation of SZU (to Ke Wang).